SCIENTIFIC REPORTS

OPEN

Maximum Entropy (Most Likely) Double Helical and Double Logarithmic Spiral Trajectories in Space-Time

Received: 14 November 2018
Accepted: 5 July 2019
Published online: 25 July 2019

M. C. Parker[1] & C. Jeynes[2]

The ubiquity of double helical and logarithmic spirals in nature is well observed, but no explanation is ever offered for their prevalence. DNA and the Milky Way galaxy are examples of such structures, whose geometric entropy we study using an information-theoretic (Shannon entropy) complex-vector analysis to calculate, respectively, the Gibbs free energy difference between B-DNA and P-DNA, and the galactic virial mass. Both of these analytic calculations (without any free parameters) are consistent with observation to within the experimental uncertainties. We define conjugate hyperbolic space and entropic momentum co-ordinates to describe these spiral structures in Minkowski space-time, enabling a consistent and holographic Hamiltonian-Lagrangian system that is completely isomorphic and complementary to that of conventional kinematics. Such double spirals therefore obey a maximum-entropy path-integral variational calculus ("the principle of least exertion", entirely comparable to the principle of least action), thereby making them the most likely geometry (also with maximal structural stability) to be adopted by any such system in space-time. These simple analytical calculations are quantitative examples of the application of the Second Law of Thermodynamics as expressed in geometric entropy terms. They are underpinned by a comprehensive entropic action ("exertion") principle based upon Boltzmann's constant as the quantum of exertion.

In 1823 Olbers formulated the problem of the dark night sky as a paradox of cosmological geometry[1], but its overriding significance to us as living beings is its functioning as an *entropy engine*[2]. Landauer's seminal work[3] (following Shannon[4] and Brillouin[5] teaches us that *information* has calculable *entropy* and obeys physical laws, while the introduction by Jaynes[6] of maximum entropy (MaxEnt) as the basis of the rules of thermodynamics (for example, the determination of the partition function) is now recognised as far-reaching. The associated variational approach to entropy production first described by Onsager[7] also provides critical insights into issues of thermodynamic reciprocity and symmetry in systems far from equilibrium.

Today, the entropic treatment of information is standard in the analysis of the efficiency of communications networks in the presence of noise[8], and it has become clear that information and its transfer are associated with discontinuities[9], implying non-adiabatic (entropy changing) conditions. Indeed, Brillouin considered information (negative entropy, or *negentropy*[5]) to be anti-correlated with entropy, and Bennett[10] showed elegantly how information *erasure* has an entropy cost: note that perfect information *copying* is excluded by the "*no-cloning theorem*"[11]. Applying *Landauer's Principle*[3] to a computation involves the *transfer* of information and therefore also results in a rise in entropy[12].

Parker & Walker[9] have also shown that holomorphic functions (which allow analytical continuation, with the sum of the Cauchy residues being zero) by themselves cannot transmit information. Instead, network stability[13] considerations require a filter function's denominator be a Hurwitz polynomial[14], resulting in the necessity for meromorphic functions (that is, complex functions analytical everywhere except at isolated poles, with a non-zero sum of Cauchy residues) being used to represent information transfer.

We will show that certain geometrical structures with simple analytical representations – the double helix and the double logarithmic spiral – can be treated formally as holomorphic; and further, we calculate their

[1]School of Computer Sciences & Electronic Engineering, University of Essex, Colchester, UK. [2]University of Surrey Ion Beam Centre, Guildford, UK. Correspondence and requests for materials should be addressed to C.J. (email: c.jeynes@surrey.ac.uk)

geometric entropy with Lagrangian methods (based on a calculus of spatial gradients) showing that the appropriate Euler-Lagrange equations are satisfied, that is, they are maximum entropy structures. Then, to verify the formalism developed, we will calculate certain observable quantities conforming to the Hamiltonian and Lagrangian equations of state and show consistency with real observations.

Holomorphic Info-Entropy

The simplest meromorphic function is functionally equivalent to an isolated singularity, that we place in a Minkowski space-time, described by basis vectors (γ_μ, $\mu \in \{0, 1, 2, 3\}$) which obey a Clifford algebra that formally distinguishes the special behaviour of the time axis γ_0, being characterized by a real time axis and imaginary space axes (see Penrose, ch.18[15]; we follow Penrose's choice of metric). An information vector h can be defined in Minkowski 4-space, and can be shown to be obtained from the sum of the temporal residues h_n associated with each spatial basis vector γ_n, $n \in \{1, 2, 3\}$, (see Appendix A Eq. A.4 in Supplementary Information) given by:

$$h = k_B \ln(x_n)\sigma^n \; n \in \{1,\ 2,\ 3\};\ \text{Einstein summation convention} \tag{1a}$$

Note that we use Einstein's summation convention in Eq. 1a (and subsequently, where stated) using tensor index notation where the lower index indicates the row and the upper the column. The bivectors $\sigma_n \equiv \gamma_n \gamma_0$ also represent unit vectors along the co-ordinate axes of the 3-dimensional space, forming a quaternion sub-algebra isomorphic to the Pauli spin vectors with the associated pseudoscalar $I = \sigma_1\sigma_2\sigma_3$, where $I^2 = -1$. Mathematically, this has transformed our starting Euclidean geometry into what will turn out to be a much more useful hyperbolic geometry. Penrose (§2.4)[15] emphasises that such a logarithmic representation is characteristic of hyperbolic geometry, and we see here its intimate relationship with entropic quantities.

We choose to define the entropy s as the Hodge-dual $*h$ of the information since this definition can be shown to have the correct properties; note that Penrose (§19.2[15]) points out that Maxwell's equations are *self-dual* in the *orthogonal complement* sense of the Hodge-dual operation, with $\sigma^m = *\sigma_n = I\sigma^n$:

$$s = k_B \ln(x_m) I\sigma^m \quad m \in \{1,\ 2,\ 3\};\ \text{summation convention} \tag{1b}$$

Thus we amplify Brillouin's assertion of the close relation of information with entropy by treating entropy mathematically as an *orthogonal complement* of information.

We choose entropic structures exhibiting a transverse helical geometry, that is, $s_3 = h_3 = 0$, with a "trajectory" axis (plane waves travelling) in the γ_3 direction. Then, given that s and h are conjugate (that is, the orthogonal complements of each other), the entropy eigenvector can be written as (for the right-handed chirality; see Appendix A Eq. A.6b in Supplementary Information)

$$s = k_B(i \ln(x_1) I\sigma^1 - \ln(x_2) I\sigma^2) \tag{2a}$$

and its (conjugate) information term similarly written as (Eqs A.7b and A.9c)

$$h = k_B(\ln(x_1)\sigma^2 - i \ln(x_2)\sigma^1) \tag{2b}$$

Note that Eqs. 1 treat the generalised singularity of an isolated pole, whereas Eq. 2 constrain this singularity into a geometry isomorphic with the double-helix implied by Maxwell's equations.

Courant & Hilbert[16] point out that the Maxwell equations are a hyperbolic version of the Cauchy-Riemann equations, and Salingaros points out that the vacuum electromagnetic (EM) field is holomorphic[17]. To form a holo-morphic info-entropy function we combine together the expressions in Eqs. 2 for information and entropy in the same way (and for the same reason) that is done in the Riemann-Silberstein[18,19] complex-vector (holomorphic) description of the EM field:

$$\underline{F} = (\underline{E} + ic\underline{B})\gamma_0 \tag{3a}$$

where $\underline{E}$ and $\underline{B}$ are the 1-vector electric and magnetic fields; $\underline{F}$ is a bivector (see Penrose[15] §19.2), hence the need for γ_0. The equivalent complex-vector for the bivector info-entropy case is:

$$f = s + Ih, \tag{3b}$$

so that we have, from Eq. 2 (see Appendix A, Eq. A.10b in Supplementary Information):

$$f = k_B \ln(x_1/x_2) I[i\sigma_1 + \sigma_2] \tag{4}$$

Note that the argument of the logarithm is now dimensionless, as is conventional. Note also that meromorphic functions are only piecewise holomorphic, so they can transmit information.

Just as Maxwell's equations have a complementary (dual, in a strong sense) helical structure of the electric and magnetic fields, we continue to choose a similar double-helical structure to the info-entropic geometry, such that the loci of the x_1 and x_2 co-ordinates of the info-entropic trajectory are related to each other by a pair of coupled differential equations:

$$x'_1 = -\kappa_0 x_2 \tag{5a}$$

$$x'_2 = \kappa_0 x_1 \tag{5b}$$

where the coupling parameter is given by $\kappa_0 \equiv 2\pi/\lambda_0$ with λ_0 being the helical pitch along the γ_3-axis (that is, the x_3 direction) and the prime indicating the differential with respect to x_3 (the trajectory axis) $x_n' \equiv \mathrm{d}x_n/\mathrm{d}x_3$ as usual.

In the entropic domain the x_3 co-ordinate plays a role analogous to that normally played by time t in conventional kinematics: to amplify this point, note that $x_0 \equiv ct$ and x_3 are also commensurate conjugates in the Pauli algebra (see Eq. A.6a in Appendix A in Supplementary Information). Considering only the functional part of the complex-vector, Eq. 4 allows us to write the 'local' geometric entropy for a double-helical structure as (Eq. A.12):

$$s = k_B \ln\left(\frac{x'_n}{\kappa_0 x^n}\right) \equiv k_B \ln W \quad n \in \{1, 2\}; \quad \text{summation convention} \tag{6}$$

which is functionally equivalent to Boltzmann's equation for entropy; where the quantity $W_n \equiv x_n'/\kappa_0 x_n$ therefore represents the number of states available for the n^{th} plane wave.

We now consider the case of the double helix in more detail, and in particular as exhibited by the structure of DNA (which is naturally right-handed). Without loss of generality, we define the locus in space l_1 of the first information-bearing helix of DNA with its axis aligned to the γ_3 direction:

$$l_1(x_3) = \gamma_1 R_0 \cos\kappa_0 x_3 + \gamma_2 R_0 \sin\kappa_0 x_3 \tag{7a}$$

where R_0, κ_0 and x_3 represent respectively the radius, pitch, and axial co-ordinate of the helix. The second helix l_2, with its complementary base-pairing and anti-parallel (C2 space group) symmetry contains the same entropic information content as l_1, but $\pi/2$ phase-shifted and propagating in the opposite (i.e. negative) γ_3 direction:

$$l_2(x_3) = \gamma_1 R_0 \sin\kappa_0 x_3 - \gamma_2 R_0 \cos\kappa_0 x_3 \tag{7b}$$

These expressions are mathematically equivalent to those for the electric and magnetic fields of an EM wave, with l_1 and l_2 being complementary. Equivalent to Eqs. 3, we now express the double-helix as the complex-vector $\sum = l_1 + il_2$ to describe a single holomorphic trajectory in Euclidean coordinates with spatial basis vectors γ_n ($n \in \{1, 2\}$):

$$\Sigma = \gamma_1 R_0 e^{i\kappa_0 x_3} - \gamma_2 i R_0 e^{i\kappa_0 x_3} \tag{8}$$

We therefore see in Eq. 8 the functionals represented by $x_1 = R_0 \exp(i\kappa_0 x_3)$ and $x_2 = -iR_0 \exp(i\kappa_0 x_3)$, from Eq. (5), where the phase and sign difference between x_1 and x_2 are typical for a pair of coupled mode equations, and which together form a holomorphic function (see Appendix B Eq. B.1 in Supplementary Information).

Hyperbolic Geometry & Entropic Momentum

We now exploit Penrose's assertion (§2.7 p.48[15]) that there is a "*hyperbolic* overall geometry of the spatial universe … the space of *velocities* … is certainly a three-dimensional hyperbolic geometry" (his italics; this assertion is underpinned by extensive observations of the cosmic microwave background). So we define for our helix the "hyperbolic position" vectors q_n in the simplest possible way that involves the logarithm characteristic of the hyperbolic geometry (see Eqs. 1), where the logarithm is kept dimensionless by the normalising (Euclidean) metric R_n (see Appendix B, Eq. B.2 in Supplementary Information):

$$\text{hyperbolic position:} \quad q_n \equiv R_n \ln(x_n/R_n) \quad n \in \{1, 2\} \tag{9a}$$

For small geometry ($x_n \ll R_n$) and for x_n having its origin at R_n such that x_n tends to $R_n + x_n$ (that is, where x_n is localised in the vicinity of R_n) the hyperbolic geometry is approximately Euclidean, $q_n \approx x_n$, and also independent of the metric R_n. For the double helix geometry we take $R_n = R_0$ for $n \in \{1, 2\}$.

The conjugate quantity for position q is the momentum p, so that moving towards a Lagrangian formalism, we therefore also define the "entropic momentum" p_n vectors in terms of an "entropic mass" m_S and the velocity q_n', where as before $q_n' \equiv \mathrm{d}q_n/\mathrm{d}x_3$. Note that q_n' is dimensionless, so that either q_n' or its inverse $1/q_n'$ can be used as a "velocity" (this ambiguity is a feature of hyperbolic velocities). It turns out that the inverse definition is more fruitful (see Appendix B, Eq. B.6):

$$\text{entropic momentum:} \quad p_n \equiv m_S/q'_n \quad n \in \{1, 2\} \tag{9b}$$

where the entropic mass m_S is defined as:

$$\text{entropic mass:} \quad m_S \equiv i\kappa_0 k_B \tag{9c}$$

and the Boltzmann constant k_B is introduced on dimensional grounds as the entropic analogue to Planck's constant in kinematics. We use the subscript 'S' as a reminder that a quantity is entropic. Clearly $i\kappa_0 k_B$ is a geometric quantity intrinsically based upon the pitch of the double helix. Simple calculus on Eq. 9a allows us to create the useful auxiliary identity $q_n' = R_n \cdot x_n'/x_n$, again highlighting the intimate relationship between Eqs 6 and 9; we will show elsewhere[20] how Liouville's theorem allows the conjugate variables p and q to be used to calculate the entropy of the geometry.

We will use Eqs. 9 as the basis for a set of Hamiltonian and Lagrangian equations. We consider first the entropic equivalent to kinetic energy, i.e. 'kinetic entropy' (KE) T_S, based upon the conventional definition of kinetic energy (Appendix B, Eq. B.8b in Supplementary Information):

$$T_S(q') = -\int p\mathrm{d}q' = -m_S \ln q' \tag{10a}$$

where the additional negative sign accounts for the inverse velocity. For the three spatial directions, we therefore have:

$$T_S = \sum_n - m_S \ln q'_n = -\tfrac{1}{2} m_S \ln(q'_n q'^n) \text{ summation convention, } n \in \{1, 2, 3\} \tag{10b}$$

We also define an entropic potential field $V_S(q)$ as a function of hyperbolic position q (the 'potential entropy'). However, for the present case of a double helix, Eq. 8 clearly represents a pair of plane waves travelling in space; which is analogous to the kinematic "free-particle" situation, such that there is therefore no associated entropic potential field, $V_S = 0$. The entropic Hamiltonian $H_S(q(x_3), p(x_3), x_3)$ is defined as usual as $H_S = T_S + V_S$, and (as shown in Appendix B, see Supplementary Information) is also a conserved quantity in hyperbolic space.

Using the canonical Legendre transformation, the entropic Lagrangian is given by (Eq. B.14):

$$\begin{aligned} L_S &= q'_n p^n - H_S \text{ summation convention, } n \in \{1, 2, 3\} \\ &= 3m_S - H_S \end{aligned} \tag{11}$$

such that the required canonical equations of state are obeyed: $\partial L_S/\partial x_3 = -\partial H_S/\partial x_3$, as well as $p'_n = \partial L_S/\partial q_n$ and $q'_n = -\partial L_S/\partial p_n$ (see Appendix B, Eqs B.15 & B.16).

Double Helix Geometry: Photons & DNA

Exertion. In analogy to the action integral (with units of J·s) we now define the *exertion* X (units of J/K) as the integration of the entropic Lagrangian L_S along the spiralling double-helical trajectory:

$$X = \int L_S \mathrm{d}l = \sqrt{1 + \kappa_0^2 R_0^2} \int L_S(q, q', x_3)\mathrm{d}x_3 \tag{12}$$

where we note the Pythagoras relationship $\mathrm{d}l/\mathrm{d}x_3 = \sqrt{1 + \kappa_0^2 R_0^2} \equiv \chi$ due to the helical geometry.

For the double-helix plane-waves description of Eq. 8, the associated entropic Lagrangian L_S has no entropic potential term (that is, $V_S = 0$) since such a system is equivalent to that of a free particle. Appendix C (Supplementary Information) provides the proof that the entropic Lagrangian functional (see Eq. C.3):

$$L_S = 3m_S + \sum_{n=1,2,3} m_S \ln q'_n = 3m_S - \sum_{n=1,2,3} m_S \ln(p_n/m_S) \tag{13a}$$

as employed in Eq. 12 satisfies the Euler-Lagrange equations

$$\frac{\mathrm{d}}{\mathrm{d}x_3}\frac{\partial L_S}{\partial q'_n} - \frac{\partial L_S}{\partial q_n} = 0\,(n \in \{1, 2, 3\}) \tag{13b}$$

demonstrating that the exertion X is at an extremum (or at least stationary) at any point along the length of the double helix since $\delta\left(\int L_S \mathrm{d}x_3\right) = 0$ (see Appendix C, Eq. C.22). Also, Appendix D (Eq. D.3b; both Appendices are in Supplementary Information) shows that the entropic Lagrangian for a double helix can be given by $L_S = 3m_S - \pi\kappa_0 k_B$; that is, in this case L_S is indeed a constant (invariant with x_3). Note also that the exertion X is scaled by the quantum of entropy, Boltzmann's constant, just as the Lagrangian itself is.

Entropy. Having defined the exertion integral, Eq. 12, we can also now see that the equivalent space-trajectory integral of the entropic Hamiltonian H_S (see Eq. 11) yields a quantity directly proportional to the entropy:

$$S = \int H_S \mathrm{d}l = \chi \int H_S(q, p, x_3)\mathrm{d}x_3 \tag{14}$$

Whereas Eq. 6 describes a 'local' entropy s, the integrated quantity S can be considered as the 'global' or the overall system entropy. Eq. 14 indicates that the overall entropy S depends not only on the centroidal trajectory of the double helix axis as described by x_3, but principally upon the spiralling path described by l with its radial dependency such that the entropy is a function of the full spatial extent (in all spatial dimensions) of the double helix structure. For convenience, we offset the entropic Hamiltonian H_S by the constant term $m_S \ln(\kappa_0 R_0)$ (see Appendix D in Supplementary Information, text prior to Eq. D.2a) which is an invariant for a double helical geometry – any Hamiltonian can be offset by a fixed (constant) amount to enable more convenient manipulation – such that the entropic Hamiltonian for a double helix can therefore be given as $H_S = \pi\kappa_0 k_B$; that is, each KE component ($n = 1, 2$) of the double helix contributes $\frac{1}{2}\pi\kappa_0 k_B$. We can also exploit the Fourier (periodic) nature of S along the double helix as characterized by the parameter $i\kappa_0$ to write the Fourier differential operator as:

$$\frac{\mathrm{d}}{\mathrm{d}x_3} \equiv i\kappa_0 \tag{15}$$

Since the Lagrangian and Hamiltonian are inversely related (through the Legendre transformation) and the exertion integral X (Eq. 12) is at an extremum (Eq. 13b), $\delta X = 0$, then the closely connected Hamiltonian trajectory integral Eq. 14 (that is, the entropy S) must also be at an extremum, $\delta S = 0$. Given that the double helix of

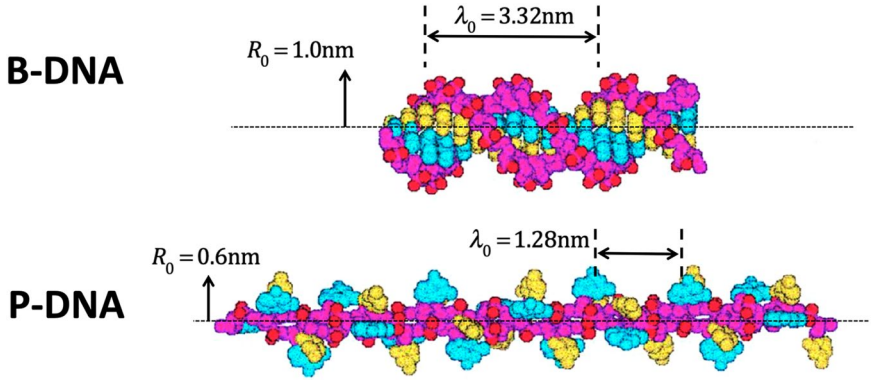

Figure 1. Two forms of DNA, with dimensions. Modified from Fig. 5 of Allemand *et al. Proc. Natl. Acad. Sci. USA* **95**, 14152–14157 (1998)[22]. Copyright (1998) National Academy of Sciences USA.

DNA represents a highly stable structure we infer from the Second Law that the entropy S is at a maximum; *ergo* the exertion X is at a minimum and the double helix topology represents a MaxEnt (most likely) trajectory in space. In summary, the overall entropy S of the double helix is given by (see Appendix D Eq. D.4):

$$S = \sqrt{(1 + \kappa_0^2 R_0^2)}\pi\kappa_0 L k_B \tag{16}$$

It is clear that the entropy S is proportional to the length L of the double helix. However, in the case of a photon its proper length is actually zero relativistically, since it travels at the speed of light: $L = 0$, therefore $S = 0$.

B-DNA and P-DNA. In an extraordinary mechanical experiment, Bryant *et al.*[21] made a controlled transformation of B-DNA to P-DNA, where the latter is an artificial form called after Linus Pauling and discussed at length by Allemand *et al.*[22] (see Fig. 1). Essentially, Bryant *et al.* held the B-DNA molecule (of length 4.681 μm) straight in tension (45 pN), and twisted it (4800 turns, with a torque of 34 pN·nm) until it had entirely transformed into the P-DNA form (with an extension of 2.8 μm). Thus, the mechanical energy expended to turn this B-DNA molecule into a P-DNA one is **1151 aJ** (126 aJ from the extension and 1025 aJ from the torque). To calculate the conformational energy changes with standard methods is computationally heavy: a recent molecular dynamics calculation by Liebl & Zacharias[23] to determine free energies actually mimicked Bryant *et al.*'s experiment.

But determining the change in structural entropy (in this context equivalent to the Gibbs free energy change) is now straightforward for these holomorphic structures. Using Eq. 16, and $\kappa_0 \equiv 2\pi/\lambda_0$, where $R_0 = \{1.0, 0.6\}$ nm respectively for the B- and P- forms; $\lambda_0 = \{3.32, 1.28\}$ nm, and $L = \{4681, 7286\}$ nm, we obtain from the geometric entropy (at 23 °C) the energies of the two forms of {244, 1428}aJ, yielding a change of **1184 aJ**. (Note that the Type A standard uncertainty just from Bryant *et al.*'s torque measurement is about 70 aJ.)

It is not entirely clear which values to assign to R_0, especially for the case of P-DNA, with plausible values for the latter ranging between 0.4 and 0.8 nm. In any case, it is clear that a very simple calculation using the apparatus of geometrical thermodynamics is capable of a result entirely consistent with experiment, where this result is not available without heavy computation using standard methods in physical chemistry.

To explain the stability of fullerene molecules a similar comparison can be made between this simple geometrical thermodynamics and the heavy computation required by the standard physical chemistry methods (which now have a very extensive literature)[24].

The Double-Armed Logarithmic Spiral

Figure 2 shows NGC 1566, an intermediate spiral galaxy 40 million light-years away in the constellation of Dorado (southern hemisphere) and the second brightest Seyfert galaxy known. The Milky Way is known to have a similar geometry (but of course we have no comparable image of it) and some parameters of our galaxy, including a double-armed logarithmic spiral, are overlaid on the Figure. We will show that such a double-armed spiral is holomorphic, just as is the double-helix of the photon or of DNA.

However, we can immediately comment on the parameters of Fig. 2, which are largely determined by the mass M_{BH} of the central galactic black hole whose entropy S_{BH} (in SI units)

$$S_{BH} = 4\pi k_B G M_{BH}^2 / c\hbar = 1.78 \times 10^{90} k_B \tag{17}$$

is given by the Bekenstein-Hawking equation: see for example Eq. 2.2 in the review of Bousso[25], or explicitly by Penrose (§27.10 p.716[15]) for a stationary black hole. As usual, $\hbar$ is the reduced Planck constant, k_B is Boltzmann's constant, and G is the gravitational constant. But it is well known that the galactic entropy is dominated by the entropy of its central super-massive black hole ($S_{MW} \approx S_{BH}$: see for example the discussion in Penrose 2010[2] §2.6 p.127), which has an equivalent black body temperature of (Bousso[25] Eq. 2.8):

$$\mathcal{T}_{BH} = \hbar c^3 / 8\pi G M_{BH} k_B = 1.5 \times 10^{-14} \mathrm{K} \tag{18}$$

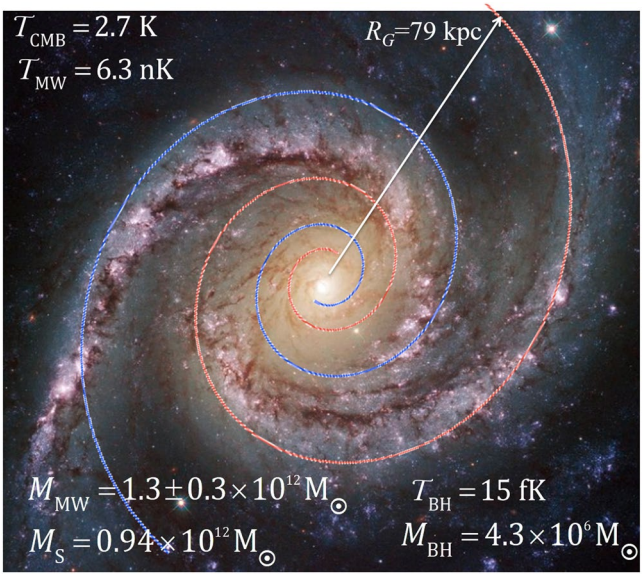

Figure 2. A spiral galaxy with an overlaid double-armed logarithmic spiral. Parameters given (see text) are of the Milky Way (MW): $\mathcal{T}_{BH}$ and M_{BH} are the (black body) temperature and mass of the super-massive black hole at the galactic centre; $\mathcal{T}_{CMB}$ is the cosmic microwave background temperature; R_G, L, $\mathcal{T}_{MW}$ are the MW radius, thickness and "temperature"; M_{MW} is the MW observed virial mass; M_S is the mass implied by the MW entropy and $\mathcal{T}_{MW}$. All masses in units of solar mass $M_\odot$. Underlying Hubble image of NGC 1566, taken 2nd June 2014 by NASA Goddard Space Flight Center https://www.flickr.com/photos/gsfc/14172908657/; licenced under CC BY 2.0 (https://creativecommons.org/licenses/by/2.0/).

M_{BH} is given by Gillessen *et al.*[26] as 4.3 ± 0.4 million solar masses $M_\odot$, where this 10% uncertainty is entirely due to the uncertainty in the galactic position of the Sun: the measurement actually has a precision better than 2% (the mass of the Sun is known very accurately, to about 10^{-4}: $M_\odot=1.989\times10^{30}$ kg). Applying this temperature to S_{MW} to obtain the energy (given by the product of entropy and temperature expressed as a mass through $E=mc^2$) we naturally recover M_{BH}.

In a standard model of the Milky Way[27] (a barred galaxy) the stellar disc is modelled as distinct "thin" and "thick" discs, with the "cut-off bulge radius" of the "thick disc" (or "bulge") given as 1.9 kpc, and the total (virial) mass within a radius of 60 kpc being $4.0\pm0.7\times10^{11}$ $M_\odot$. Rix & Bovy[28] explain that there is no well defined distinction between the "thin" and "thick" discs, but the characteristic "scale height" of the "thin disc" can be given approximately as 0.3 kpc. Patsis *et al.*[29] show that the "bar" (bulge) of the galaxy can be described in orbital dynamics terms, and Saito *et al.*[30] map the bulge (the "bar") from observational data. We will assume an approximate galactic half-thickness $L/2=1$ kpc. The *parsec* is defined as the distance from the Sun of a star observed to have one second of arc annual stellar parallax, and is therefore relative to the diameter of Earth's orbit ($1\,\text{kpc}=3.09\times10^{19}$ m).

Another study has concentrated on the galactic mass[31]: giving the observed stellar galactic mass and the virial mass respectively as $6.4\pm0.6\times10^{10}\,M_\odot$, and $1.26\pm0.24\times10^{12}\,M_\odot$. "Virial" mass includes so-called "dark matter" and is derived from the observations of stellar proper motions in large scale star surveys using the Virial Theorem (Clausius, 1870).

Consider a doubled-armed logarithmic spiral, as frequently observed for galaxies (see Fig. 2 which is a plan view projecting the 3-D object onto a plane). Here, the holomorphic functionals describing the x_1 and x_2 locus co-ordinates are now (in contrast to Eq. 8):

$$x_1=R_Ge^{-\Lambda(x_3+L/2)}e^{i\kappa x_3}=r_{BH}e^{-\Lambda x_3}e^{i\kappa x_3}\text{ and }x_2=-iR_Ge^{-\Lambda(x_3+L/2)}e^{i\kappa x_3}=-ir_{BH}e^{-\Lambda x_3}e^{i\kappa x_3} \tag{19}$$

such that the instantaneous radius is $R_n=R_Ge^{-\Lambda(x_3+L/2)}=r_{BH}e^{-\Lambda x_3}$ for $n=1, 2$ (see Eq. B.24 in Appendix B), where r_{BH} is the Schwarzschild radius (the event horizon) of the central black hole. The logarithmic radial parameter Λ is given by the requirement that the galactic radius R_G and the Schwarzschild radius r_{BH} are related logarithmically by the half-thickness $L/2$ (see Eq. D.15a in Appendix D, Supplementary Information): $r_{BH}=R_G\exp(-\Lambda L/2)$, or

$$\Lambda=(2/L)\times\ln(R_G/r_{BH}) \tag{20}$$

where for the Milky Way $\Lambda=26\,\text{kpc}^{-1}$. The radius r_{BH} of the central galactic black hole is determined by the black hole mass M_{BH} to be 1.270×10^7 km (about 18 times the solar radius; see Eq. D.14). The coupling coefficient κ is assumed to vary similarly to the radius, that is $\kappa=\kappa_{BH}\exp(\Lambda x_3)$ (Eq. B.24d), where κ_{BH} is the pitch at the black hole event horizon. The associated hyperbolic co-ordinates (using Eq. 9a, see Eq. B.33) are:

$$\begin{aligned} q_1 &= ir_{BH}e^{-\Lambda x_3}\kappa x_3 \\ q_2 &= ir_{BH}e^{-\Lambda x_3}(\kappa x_3 - \pi/2) \\ q_3 &= x_3 \end{aligned} \tag{21}$$

All quantities clearly revert to their respective double-helical quantities when the logarithmic spiral parameter $\Lambda = 0$. We find that a logarithmic spiral is associated with an entropic potential field $V_S \neq 0$ causing a hyperbolic acceleration; indeed, as the entropic analogy to Newton's second law of kinematics ($F = m\ddot{x}$), we solve the Euler-Lagrange equations (defined in hyperbolic space q_n) $\mathrm{d}p_n/\mathrm{d}x_3 = -m_S q_{n''}/q_{n'} = -\partial V_S/\partial q n_2$, where the final term in the equation (the entropic potential gradient) is therefore equivalent to the entropic force F_S. The associated entropic acceleration is given by $\Gamma_n = -q_{n''}/q_{n'2}$, the minus sign being due to the inverse velocity nature of q'. The proof that the double-armed logarithmic spiral satisfies the Euler-Lagrange equations in hyperbolic space q (that is, obeys the principle of *least exertion*) is given in Appendix C (Eq. C.47, see Supplementary Information).

In Euclidean (x) space, we find that the entropic potential field V_S for the logarithmic double spiral is expressed as (see Eq. B.42 in Appendix B, Supplementary Information; K_0 and K_3 are dimensionless):

$$V_S(x) = \frac{im_S K_0 e^{i\kappa_G x_3}}{1 - \Lambda x_3}\left(\frac{x_1 + ix_2}{x_1 x_2}\right) - \frac{m_S K_3 e^{\Lambda x_3}}{R_3(1 - \Lambda x_3)} \tag{22}$$

It is indeed interesting to note the existence of an inverse-square law (in Euclidean space) for the γ_1 and γ_2 directions at the heart of this entropic potential field; the entropic force varies as

$$F_{S,n} = -\frac{\partial V_S}{\partial x_n} = -\frac{m_S K_0 e^{i\kappa_G x_3}}{x_n^2(1 - \Lambda x_3)} \quad n = 1, 2 \tag{23}$$

that is, $F_{S,n} \propto {x_n}^{-2}$, with F_S also being proportional to the entropic mass m_S assumed located at the centre of the system and to be the cause of the entropic potential field. We emphasise, however, that although Eqs 22 and 23 express the entropic field in a more intuitive Euclidean form, the entropic Hamiltonian and Lagrangian equations are only correctly applied in hyperbolic space.

The general shape of the Milky Way is closely determined by these holomorphic logarithmic spirals. In particular, it can be shown that the ratio of the extremal radius R_G to the full-thickness L is (see Appendix D, Eq. D.17, Supplementary Information):

$$R_G/L = 4\pi^2 \tag{24}$$

The radius R_G is rather poorly defined observationally, and the estimate $L/2 = 1$ kpc given above implies (from Eq. 24) $R_G = 79$ kpc, which is within the range usually given: therefore Eq. 24 has some observational support. The Milky Way in reality has a complex structure involving multiple spiral arms, a central "bulge", and oscillating star densities reported recently[32] as persisting to much larger distances than R_G. None of this is considered in our zeroth order model. The present treatment should also be regarded as a static approximation neglecting the dynamic mechanisms of galactic formation and evolution. Figure 2 shows only the plan view of the model: the galactic cross-section is here modelled as a disc of essentially uniform thickness L, dimpled at its centre (that is, ignoring the "bulge" altogether).

The spiral coordinate x_3 projected onto the plane in Fig. 2 is associated with an azimuthal angle $\theta = \kappa_G x_3$ where the appropriate wavelength scale λ_G for the galaxy is given by the galactic wavenumber $\kappa_G = 2\pi/\lambda_G$. This can be calculated from the galactic structural entropy S, well approximated by (Appendix D, Eq. D.13b, Supplementary Information):

$$S = A\kappa_G^2 k_B/2 \tag{25}$$

where $A \equiv 2\pi\, R_G\, L$ closely approximates the area of an ellipsoid of radii $L/2$ and R_G. Eq. 25 for the logarithmic spiral is exactly equivalent to Eq. 16 for the double-helix. Thus we get an expression for the galactic wavelength λ_G (see Eq. D.16 in Appendix D)

$$\lambda_G = (2\pi \cdot l_P/r_{BH}) \cdot \sqrt{(R_G L)} = 1.059 \times 10^{-24}\mathrm{m} \tag{26}$$

where $l_P = 1.616 \times 10^{-35}$ m is the Planck length.

Eq. 25 is startling. The galactic entropy (which is almost exactly the central supermassive black hole entropy) is given "holographically" (see Appendix D, Eq. D.5 and subsequent discussion) by the surface area of the galaxy, just as the black hole entropy is determined by the surface area of the event horizon. We now postulate that just as for the black hole, a "temperature" $\mathcal{T}_{MW}$ can be defined at this holographic surface. This temperature must lie between the central supermassive black hole temperature (15 fK) and the cosmic microwave background temperature of 2.73 K.

To obtain a reasonable estimate of $\mathcal{T}_{MW}$ we note that the power radiated from a spherical black body surface of radius R and temperature $\mathcal{T}$ is $4\pi\sigma\,(R\mathcal{T}^2)^2$, where σ is the Stefan-Boltzmann constant. We therefore highlight here the appearance of the composite quantity $R\mathcal{T}^2$ that appears as a consequence of the Stefan-Boltzmann law. With both R and $\mathcal{T}$ increasing exponentially with distance from the galactic centre, it is clear the resulting large temperature gradient along x_3 implies a large energy flow towards and into the black hole: the galaxy is not in

Quantity	Kinematic (Conventional)	Entropic Equivalent	See near Eqs
Physical constant	Planck, $\hbar$ [Js]	Boltzmann, k_B [JK^{-1}]	9c, 12
Space-time co-ordinates, q	$x_1, x_2, x_3, x_0\ (\equiv ct)$ (Euclidean, Minkowski)	$q_n = R_n \ln\left(\frac{x_n}{R_n}\right)$ (hyperbolic, Minkowski)	1, 9a, 21
Differential operator	$\nabla = \partial/\partial x_n$	$\nabla_q = \partial/\partial q_n$	11
Wavelength, λ & wavenumber κ	$\lambda(=2\pi c/\omega)$ & $k = 2\pi/\lambda$	λ = helical pitch; $\kappa = 2\pi/\lambda$	5
Time-like axis & associated Fourier differential	$t,\ \frac{\mathrm{d}}{\mathrm{d}t} \equiv i\omega$	$x_3,\ \frac{\mathrm{d}}{\mathrm{d}x_3} \equiv i\kappa$	11, 15
Momentum, p	$p = m\dot{x} = \frac{2\pi\hbar}{\lambda}$	$p = m_S v^{-1} = \frac{m_S}{q'} = \frac{k_B}{R}$	9b, 10
Velocity, v	$\dot{x}_n = \frac{\mathrm{d}x_n}{\mathrm{d}t} \quad n = 1, 2, 3$	$v\&v^{-1} \equiv q'_n = \frac{\mathrm{d}q_n}{\mathrm{d}x_3} = R_n \frac{x'_n}{x_n}$ (i.e. also has inverse velocity, v^{-1}, characteristics)	9b, 10
Mass, m	$m\left(\equiv\frac{k\hbar}{c}\right)$ [kg]	$m_S \equiv i\kappa k_B$ [JK^{-1}m^{-1}]	9c, 15
Kinetic term $T = \int p\mathrm{d}v$	$T = \int p\mathrm{d}\dot{x} = \frac{1}{2} m\dot{x}^2$	$T_S = -\int p\mathrm{d}q' = -m_S \ln q' = \frac{1}{2} m_S \ln q'^2$	10
Potential term, V	$V = m\ddot{x}x \equiv mgx$	$V_S(q) = m_S(-q''/q'^2)q \equiv m_S\Gamma q$	11, 22
Hamiltonian, H	$H = T + V$	$H_S = T_S + V_S = \sum_{n=1}^{3} -m_S \ln q'_n + V_S(q_n)$	11
Lagrangian, L	$L = \sum_{n=1}^{3} p_n \dot{x}_n - H = T - V$	$L_S = \sum_{n=1}^{3} p_n q'_n - H_S = 3m_S - H_S$	11, 13a
Newton's 2nd Law: [Euler-Lagrange formulation]	$\frac{\mathrm{d}}{\mathrm{d}t}\frac{\partial L}{\partial \dot{x}_n} - \frac{\partial L}{\partial x_n} = 0$	$\frac{\mathrm{d}}{\mathrm{d}x_3}\frac{\partial L_S}{\partial q'_n} - \frac{\partial L_S}{\partial q_n} = 0$	13b, 21
$F = ma$	$F = -\nabla V = m\ddot{x}$	$F_S = -\nabla_q V_S = -m_S q''/q'^2 = m_S\Gamma$	21, 23
Acceleration	$\ddot{x} = g$[ms^{-2}]	$-q''/q'^2 = \Gamma$ [m^{-1}]	21, 23
Action/Exertion Integral	$\mathcal{A} = \int L\mathrm{d}t$ [$\hbar$]	$X = \chi \int L_S \mathrm{d}x_3$ [k_B]	12
Variational Principle	$\delta\mathcal{A} = \delta\int L\mathrm{d}t = 0$, Least Time/Action	$\delta X = 0,\ \delta\int L_S \mathrm{d}x_3 = 0$, Least Exertion	12, 13b
Entropy	$S = \int \frac{\mathrm{d}E}{\mathcal{T}}$	$S = \chi \int H_S \mathrm{d}x_3$	14, 16, 25
Maximum Entropy	$\delta\int H\mathrm{d}t = 0$, Stationary Phase (Group Velocity)	$\delta S = 0, \quad \delta\int H_S \mathrm{d}x_3 = 0$	15

Table 1. Isomorphism between kinematic and entropic quantities.

thermal equilibrium! However, to at least maintain some thermal 'stability' along the γ_3 axis, we might assume that $\mathcal{T}^2$ varies similarly to R, so that the black body power inwardly radiated from each spherical surface along the γ_3 axis maintains some continuity. Relying on the isomorphism between the double-helix and the logarithmic double-spiral in hyperbolic space we therefore consider $\mathcal{T}^2$ to vary with $\exp(-\Lambda x_3)$ just as R and the galactic wavelength λ do (see Eq. 19 and Eq. B.24 in Appendix B):

$$R = r_{BH}\exp(-\Lambda x_3) \tag{27a}$$

$$\mathcal{T} = \mathcal{T}_{BH}\exp(-\Lambda x_3/2) \tag{27b}$$

Then, at $x_3 = -L/2$ with $\Lambda = 26\,\mathrm{kpc}^{-1}$, we have $\mathcal{T} = \mathcal{T}_{MW} = 6.3\,\mathrm{nK}$ for $L = 2\,\mathrm{kpc}$ giving $M_{\mathrm{MW}} = 0.94 \times 10^{12}\,\mathrm{M}_\odot$ (and $R_G = 79\,\mathrm{kpc}$) consistent with observation. To obtain the central observed value for the virial mass of the Milky Way of $M_{\mathrm{MW}} = 1.26 \times 10^{12}\,\mathrm{M}_\odot$, we need $L = 3.6\,\mathrm{kpc}$ (giving $R_G = 142\,\mathrm{kpc}$ and $\mathcal{T}_{MW} = 8.4\,\mathrm{nK}$).

To summarise: we have shown that the structure of the galaxy for which we have detailed experimental observations (that is, the Milky Way) is consistent with a holomorphic representation in geometric algebra. In particular, we have shown that the galactic *shape*, *aspect ratio*, and *structural stability* (which are all highly constrained by the algebra) are consistent with observation; and we have also shown that the total galactic *mass* is also consistent with observation. Note that this is a simplified ("zeroth order") analytical approximation to reality: for example, the black hole angular momentum is neglected, as are the dynamics driving the galactic evolution. Also, we have not started to consider the perturbation problem implied by deviations of the star population from the ideal logarithmic spiral; although we would anticipate that the principle of least exertion causes an entropic force to be exerted so as to maintain the MaxEnt galactic structure.

Notwithstanding the approximations, these results are very surprising, because they underline the dominant effect that the central super-massive black hole has on the galactic structure. In fact, this treatment gives the proper weight to the effect of the black hole entropy, which is certainly not hidden away behind the event horizon.

Isomorphism between Mechanics and Entropy

Table 1 shows the multiple isomorphisms that exist between kinematic and entropic quantities revealed by our treatment. There has been significant recent interest in comparable methods. Baez & Pollard[33] argue for an "analogy" between thermodynamics and quantum mechanics, giving rise to a quantity they call "quantropy" (quantum entropy, which they call "mysterious"). They also give a Table of "analogies" between statistical and quantum dynamics comparable to our Table of isomorphisms. We believe that our results confirm and extend this approach.

Velazquez[34] has also tabulated some consequences of the complementarity of the Planck and Boltzmann constants. Dixit *et al.*[35] have reviewed the use of "Maximum-Caliber" to characterise trajectories ("world-lines") in non-equilibrium thermodynamics (where "*caliber*" is a term introduced by Jaynes[36] to characterise the evolution in space-time of the ensemble of trajectories of microstates; it is proportional to our "*Exertion*").

Considering Table 1, we have already observed that the hyperbolic Minkowski space (generated through the normalising Euclidean metric, R_n) is the entropic analogue to the Euclidean Minkowski space of kinematics, with consequent del operators; that Boltzmann's constant is the entropic quantum analogue to Planck's quantum of action (also pointed out by Córdoba *et al.*[37]) with consequently analogous definitions for momentum; and that the helical pitch (or wavelength) implies the space-like entropic analogue of time in kinematics. As we have seen, this latter also implies holographic properties of the treatment (that is, properties of an area being fully equivalent to parameters of a volume).

Both mass and its entropic equivalent m_S have natural units of inverse length, but m_S is imaginary as a consequence of the holomorphism (Eq. 9c). The parameter Λ describing a logarithmic spiral contributes to the entropic (hyperbolic) acceleration Γ as a consequence of an entropic force, in analogy to Newton's 2nd Law; and the double-helix can be seen as a special case ($\Lambda = 0$) of the double-armed logarithmic spiral. The Hamiltonian and Lagrangian formulations then follow equivalently for both energy and entropy, with the *Exertion* integral equivalent to the classical *Action* integral, both obeying the principle of stationary "action".

Summary

Formal mathematics establishes tautologies which are frequently very surprising, and we have used well-established formal methods in a properly quantitative treatment of entropy, revealing that measurable (and measured) quantities from the molecular to the galactic scale can be readily calculated in a simple analytical treatment. We have considered systems of high symmetry which are amenable to our simplified analytical approach, but we expect the method to be readily generalisable to more complex systems.

The computational demands of conformational chemistry are very severe; perhaps this approach will stimulate algorithmic advances to speed the calculations for static problems, or even to address dynamic geometrical problems (like protein folding) in new ways?

We have used a "toy" model of the Milky Way, which ignores the central "bulge" and multiple arms, but a more realistic model already available would simply take a linear combination of a spherical central feature[24] and multiple double-spiral arms. The difficulty here is not in the modelling but in the choice of realistic observational data for the model parameters.

References

1. Harrison, E. R. Olbers' Paradox. *Nature* **204**, 271–272 (1964).
2. Penrose, R. *Cycles of Time* (The Bodley Head, 2010).
3. Landauer, R. Computation: A fundamental physical view. *Physica Scripta* **35**, 88–95 (1987).
4. Shannon, C. A mathematical theory of communication. *Bell System Technical Journal* **27**(379–423), 623–656 (1948).
5. Brillouin, L. *Science & Information Theory* (Academic, 1956).
6. Jaynes, E. T. Information theory and statistical mechanics. *Physical Review* **106**, 620–630 (1957).
7. Onsager, L. Reciprocal relations in irreversible processes I. *Physical Review* **37**, 405–426 (1931).
8. Parker, M. C. & Walker, S. D. A Unified Carnot Thermodynamic and Shannon Channel Capacity Information-Theoretic Energy Efficiency Analysis. *IEEE Transactions on Communications* **62**, 3552–3559 (2014).
9. Parker, M. C. & Walker, S. D. Information transfer and Landauer's principle. *Optics Communications* **229**, 23–27 (2004).
10. Bennett, C. H. Demons, Engines and the Second Law. *Scientific American* **257**, 108–116 (1987).
11. Wootters, W. K. & Zurek, W. H. A single quantum cannot be cloned. *Nature* **299**, 802–803 (1982).
12. Parker, M. C. & Walker, S. D. Is computation reversible? *Optics Communications* **271**, 274–277 (2007).
13. Bose, N. K. Argument conditions of Hurwitz and Schur polynomials from network theory. *IEEE Transactions on Automatic Control* **39**, 345–346 (1994).
14. Hurwitz, A. Ueber die Bedingungen, unter welchen eine Gleichung nur Wurzeln mit negativen reellen Theilen besitzt. *Mathematische Annalen* **46**, 273–284 (1895).
15. Penrose, R. *The Road to Reality* (Jonathan Cape 2004).
16. Courant, R. & Hilbert, D. *Methods of Mathematical Physics* (Interscience - Wiley, New York, vol.II p.178 (1962).
17. Salingaros, N. Electromagnetism and the holomorphic properties of spacetime. *J. Math. Phys.* **22**, 1919–1925 (1981).
18. Bialynicki-Birula, I. Photon Wave Function in *Progress in Optics XXXVI* (ed. Wolf, E.) 245–294 (Elsevier, Amsterdam, 1996).
19. Bialynicki-Birula, I. & Bialynicka-Birula, Z. The role of the Riemann–Silberstein vector in classical and quantum theories of electromagnetism. *J. Phys. A: Math. Theor.* **46**, 053001 (32pp) (2013).
20. Parker, M. C. & Jeynes, C. Entropic Uncertainty Principle and Holographic Principle derived from Liouville's Theorem. *J. Phys. A* (in review 2019).
21. Bryant, Z. *et al.* Structural transitions and elasticity from torque measurements on DNA. *Nature* **424**, 338–341 (2003).
22. Allemand, J. F., Bensimon, D., Lavery, R. & Croquette, V. Stretched and overwound DNA forms a Pauling-like structure with exposed bases. *Proc. Natl. Acad. Sci. USA* **95**, 14152–14157 (1998).
23. Liebl, K. & Zacharias, M. Unwinding Induced Melting of Double-Stranded DNA Studied by Free Energy Simulations. *J. Phys. Chem. B* **121**, 11019–11030 (2017).
24. Parker, M. C. & Jeynes, C. Fullerene Stability by Geometrical Thermodynamics. *Physical Chemistry Chemical Physics* (in review 2019).
25. Bousso, R. The Holographic Principle. *Reviews of Modern Physics* **74**, 825–874 (2002).
26. Gillessen, S. *et al.* Monitoring stellar orbits around the massive black hole in the galactic centre. *The Astrophysical Journal* **692**, 1075–1109 (2009).
27. Bovy, J. galpy: A python library for galactic dynamics. *The Astrophysical Journal Supplement Series*, **216**, 29 (27pp) (2015).
28. Rix, H.-W. & Bovy, J. The Milky Way's stellar disk: Mapping and modeling the Galactic disk. *The Astronomy and Astrophysical Review* **21**, 61–118 (2013).
29. Patsis, P. A., Skokos, Ch & Athanassoula, E. Orbital dynamics of three-dimensional bars – III. Boxy/peanut edge-on profiles. *Monthly Notices of the Royal Astronomical Society* **337**, 578–596 (2002).
30. Saito, R. K. *et al.* Mapping the X-shaped Milky Way Bulge. *The Astronomical Journal* **142**, 76 (6pp) (2011).
31. McMillan, P. J. Mass models of the Milky Way. *Monthly Notices of the Royal Astronomical Society* **414**, 2446–2457 (2011).

32. Xu, Y *et al*. Rings and Radial Waves in the Disk of the Milky Way. *The Astrophysical Journal*, **801**, 105 (25pp) (2015).
33. Baez, J. C. & Pollard, B. S. Quantropy. *Entropy* **17**, 772–789 (2015).
34. Velazquez Abad, L. Principles of classical statistical mechanics: A perspective from the notion of complementarity. *Annals of Physics* **327**, 1682–1693 (2012).
35. Dixit, P. D. *et al*. Perspective: Maximum caliber is a general variational principle for dynamical systems. *The Journal of Chemical Physics*, **148**, 010901 (10 pp) (2018).
36. Jaynes, E. T. The minimum entropy production principle. *Annual Review of Physical Chemistry* **31**, 579–601 (1980).
37. Córdoba, P. F., Isidro, J. M. & Perea, M. H. Emergence from irreversibility. *Journal of Physics: Conference Series* **442**, 012033 (2013).

Acknowledgements

Information and comments from Prof.M.Gieles, Dr. J.C.G. Jeynes and D. Glass are acknowledged.

Author Contributions

M.C.P. developed the physics and wrote the paper; C.J. critically discussed the physics, helped develop it, and wrote and edited the paper.

Additional Information

Supplementary information accompanies this paper at https://doi.org/10.1038/s41598-019-46765-w.

Competing Interests: The authors declare no competing interests.

Publisher's note: Springer Nature remains neutral with regard to jurisdictional claims in published maps and institutional affiliations.